



## Early leaf senescence reveals drought stress thresholds and mortality risk across temperate forests

Pia Labenski<sup>1</sup>, Allan Buras<sup>2</sup>, Rüdiger Grote<sup>1</sup>, Martin Thurner<sup>1</sup>, Nadine K. Ruehr<sup>1</sup>

<sup>1</sup> Institute of Meteorology and Climate Research Atmospheric Environmental Research (IMKIFU), Karlsruhe Institute of Technology (KIT), 82467 Garmisch-Partenkirchen, Germany

<sup>2</sup> Land-Surface-Atmosphere Interactions, Technical University of Munich (TUM), 85354 Freising, Germany

Correspondence to: Pia Labenski ([pia.labenski@kit.edu](mailto:pia.labenski@kit.edu))

**Abstract.** Drought-induced early leaf senescence is increasingly widespread in temperate forests, yet the thresholds triggering this response and whether it reflects adaptive drought avoidance or progressive stress remain poorly constrained. Combining six years (2018–2023) of Sentinel-2 observations with atmospheric and soil drought indicators and canopy mortality maps across German beech (*Fagus sylvatica*) and oak (*Quercus robur*, *Q. petraea*) forests, we show that early senescence emerges once cumulative drought stress exceeds species-specific hydraulic thresholds. Sustained atmospheric vapour pressure deficit (VPD) followed by late-summer soil water depletion sharply increases senescence probability, with critical thresholds occurring after six consecutive weeks of daily maximum VPD above 1.9 kPa in beech and 2.1 kPa in oak, and after two weeks of root-zone soil water potential ( $\psi_{\text{soil}}$ ) below  $-0.8$  MPa (beech) and  $-0.9$  MPa (oak). Sensitivity differs between forest types: beech-dominated stands respond more strongly to soil drought, whereas oak stands are more sensitive to atmospheric drought. Elevated spring VPD further amplifies early senescence risk in both species, pointing to cross-seasonal legacy effects in canopy stress responses. Critically, early senescence – and particularly its recurrence across consecutive years – is associated with significantly elevated canopy mortality, indicating progressive hydraulic stress rather than protective drought avoidance. Clustering forests by senescence dynamics and mortality outcomes reveals distinct drought-response types ranging from resistant stands buffered by favourable soil and climate conditions to vulnerable lowland forests with elevated mortality risk. Together, these results establish early leaf senescence as a landscape-scale indicator of drought stress severity and emerging mortality risk, providing a new framework for identifying forest vulnerability under intensifying climate extremes.

### 1 Introduction

Recent hot droughts have exposed European temperate forests to exceptional stress, with the 2018–2022 sequence reaching unprecedented levels of drought intensity, persistence, and spatial extent across the continent (Bevacqua et al., 2024; Rakovec et al., 2022). These conditions led to widespread declines in forest health, particularly in Central Europe (George et al., 2022; Knutzen et al., 2025; Schuldt et al., 2020). One of the earliest and most widespread responses was premature leaf coloration and shedding in deciduous forests during the summer of 2018, in some areas starting as early as late July (Buras et



al., 2020; Obladen et al., 2021; Schuldt et al., 2020). Early leaf senescence affected an estimated 11% of Central European forests that year (Brun et al., 2020) and recurred during subsequent drought summers (Descals et al., 2023). Such shifts in leaf phenology can profoundly impact ecosystem processes by altering the timing and magnitude of carbon, water, and nutrient fluxes (Piao et al., 2019; Richardson et al., 2013). Yet, the drought conditions triggering this response, the physiological thresholds involved, and its implications for forest resilience remain poorly constrained, posing a key challenge in predicting ecosystem responses to climate extremes.

While recent studies have established that drought drives senescence advancement globally (Ma et al., 2024; Yan et al., 2025; Zhang et al., 2025), their coarse spatial resolution and reliance on broad climate indices limit the identification of species-specific drought thresholds governing early canopy decline across different forest types. This is critical because senescence responses vary substantially across species, sites, and years (Bigler & Vitasse, 2021; Bréda et al., 2006; Leuzinger et al., 2005; Zuccarini et al., 2023), indicating that early senescence is driven by physiological stress thresholds that differ across species. For instance, drought-induced leaf shedding is well documented in European beech (Bréda et al., 2006; Leuschner, 2020), whereas responses of temperate oaks are more variable, depending on drought intensity, timing, and re-watering (Günthardt-Goerg et al., 2013; Spieß et al., 2012; Vander Mijnsbrugge et al., 2016). Forest composition and structure, soil properties, and terrain further modulate senescence responses at the regional scale (Brun et al., 2020; Meier et al., 2021). For beech, critical soil water potential thresholds triggering leaf shedding have been identified at the stand scale (Walthert et al., 2021), but comparable hydraulic thresholds remain lacking for oak and have not been quantified at landscape scale for either species.

Mechanistically, drought-induced early senescence may reflect either an adaptive response – limiting water loss and protecting the hydraulic system from embolism at the cost of reduced carbon assimilation (Nadal-Sala et al., 2021; Quetin et al., 2026; Wolfe et al., 2016) – or a symptom of cumulative damage, including xylem embolism or heat-induced tissue injury (Scafaro et al., 2021; Walthert et al., 2021). Following the 2003 drought, early senescence in beech was not associated with crown deterioration (Bréda et al., 2006), suggesting a protective response. However, more recent evidence indicates that early senescence is increasingly associated with lasting hydraulic damage. Although measurements of nutrient dynamics in prematurely senescing leaves suggest a controlled physiological process that may initially function as a protective response (Schuldt et al., 2020), legacy effects following the 2018 drought included increased crown dieback and lagged tree mortality in early senescing beech, which has been linked to persistent xylem embolism limiting water supply in the following year (Arend et al., 2022; Frei et al., 2022; Walthert et al., 2021). If hydraulic function remains impaired or trees with reduced leaf area cannot maintain a positive carbon balance, a steady decline of tree vigour can be expected particularly under recurrent droughts (Hájíčková et al., 2024; Salmon et al., 2015). Resolving whether early senescence primarily reflects drought avoidance or progressive damage is therefore essential for predicting forest resilience and mortality risk.

Recent advances in high-resolution spatial datasets now enable addressing these questions at landscape scale. Sentinel-2 time series allow spatially continuous monitoring of canopy phenology across the 2018–2022 drought sequence in Central Europe, while recently available high-resolution tree species maps and mortality datasets enable species-specific analyses of



forest canopy responses. Here, we combine satellite-derived observations of leaf senescence with atmospheric and soil drought indicators to quantify the drivers and consequences of early leaf senescence in temperate forests. We focus on deciduous forests across Germany, which were among the most severely affected by the 2018–2022 drought sequence, and on two dominant tree species with contrasting hydraulic strategies: European beech (*Fagus sylvatica*) and oak (*Quercus*  
70 *robur*, *Q. petraea*). We identify species-specific drought thresholds governing the emergence of premature canopy senescence, assess whether early senescence is linked to increased canopy mortality, and characterise spatial patterns of drought vulnerability across these forests. By linking satellite-observed phenology to physiologically meaningful drought indicators and mortality outcomes, this study establishes early leaf senescence as a landscape-scale indicator of cumulative drought stress and emerging mortality risk, and provides a new framework for monitoring and anticipating forest  
75 vulnerability under future climate extremes.

## 2 Methods

### 2.1 Satellite-based mapping of senescence onset

#### 2.1.1 Sentinel-2 time series processing

We used Level 2 Analysis Ready Data (ARD) from Sentinel-2 at 10 m resolution covering Germany for the years 2018–  
80 2023, available via the EO-Lab platform (<https://eo-lab.org/>). The ARD were generated using the FORCE software (Frantz, 2019), and included cloud and cloud shadow masking, atmospheric, topographic, and additional radiometric corrections, and finally data cubing. Quality Assurance Information (QAI) flags generated by the FORCE Level-2 processing system were used to remove pixels with snow, frozen conditions, or affected by sensor saturation. For further analysis, we included only  
85 10 m pixels classified as dominated by either European beech or oak species (*Quercus robur* and *Quercus petraea*, available only in a combined *Quercus* class) according to a national 10 m tree species map (Blickensdörfer et al., 2024), and with  
>70% canopy cover according to the Copernicus tree cover density product (Copernicus, 2024), to minimize the influence of understory vegetation on the spectral signal.

Using the FORCE time series analysis module (Frantz, 2020b), we computed four vegetation indices (VIs) – three red-edge-based VIs and the NDVI (Table S1) – as candidate VIs for estimating senescence onset (SO). Outliers in the time series were  
90 removed via residual-based filtering with linear interpolation of observation triplets (Frantz, 2020a). The filtered time series were interpolated using a Radial Basis Function (RBF) filter with three different kernel widths to generate weighted moving window averages based on local data availability (Schwieder et al., 2016), resulting in a daily time series. Residual noise was further reduced by fitting piecewise cubic splines that capture seasonal dynamics.

SO was estimated from the smoothed VI time series as the day of year (DoY) when the signal dropped below different  
95 candidate seasonal amplitude thresholds (90%, 85%, 80%, 75%, 70%) after the summer maximum. Forest areas affected by



disturbance events (fires, windthrows, bark beetle outbreaks, salvage logging) were excluded for the affected year using the European Forest Disturbance Atlas (Viana-Soto & Senf, 2025).

### 2.1.2 Validation against ground observations

We compared satellite-derived SO estimates to plot-level phenological observations for beech and oak on ICP Forests Level II plots (Fleck et al., 2016). For this, we extracted mean SO values from Sentinel-2 pixels classified as beech- or oak-dominated and spatially overlapping the plots (assumed area: 0.25 ha, the minimum requirement for Level II plots) and correlated these with field-recorded dates for coloration and litterfall onset. We used different spatial aggregation levels for the remotely sensed SO estimates to reduce noise in pixel-level time series and to evaluate scale effects on the agreement between satellite-based estimates and observations. In total, 20 ICP Forests plots were included, however, incomplete phenological records resulted in averages of 11 beech and four oak plot observations per year (Figure S1). Field observations refer to the first occurrence of ‘infrequent or slight’ canopy coloration or litterfall (1-33% of the canopy affected; Raspe et al., 2020a), estimated from plot-level canopy assessments. We focused on this early phenological stage rather than later ones to capture the initial effects of drought on canopy phenology. We then selected the VI and amplitude threshold that minimized the RMSE between satellite-derived and field-recorded SO across all years, sites, species, and spatial aggregation levels. Satellite-derived SO showed moderate agreement with field observations of leaf coloration and litterfall onset, with correlations of  $r=0.43$  and  $r=0.34$  at the finest aggregation scale (50x50 m; minimum ICP Forests plot size), respectively. Among the tested indices and thresholds, the normalized difference red-edge index (NDRE) using an 80 % seasonal amplitude threshold consistently produced the closest correspondence with field observations across different aggregation scales (Figure S2), and was therefore used to derive annual senescence maps for subsequent analyses. Spatial aggregation improved the agreement with field observations by reducing pixel-level noise from data gaps, residual atmospheric effects, geolocation uncertainty, and small-scale canopy heterogeneity, but also reduced variability in the satellite-derived SO estimates due to signal averaging. Alternative approaches, including derivative-based estimation of SO (cf. Misra et al., 2016) or using later phenological categories (‘common or moderate’; 33-66% of the canopy affected), were also tested but did not improve agreement (Figure S3). Despite some underestimation of very early senescence events, the satellite-derived SO captured the overall variability in canopy senescence across beech- and oak-dominated forests (Figures S1-S2). The comparison with field data is further discussed in Supplementary Note 1.

### 2.1.3 Early senescence definition and map preparation

We defined early senescence onset ( $SO_{\text{early}}$ ) as occurring before DoY 244 (1 September in normal years, 31 August in leap years), consistent with previous studies (e.g. Descals et al., 2023), and classified later dates as normal senescence onset ( $SO_{\text{normal}}$ ). We also explored an anomaly-based definition of early leaf senescence similar to Bigler & Vitasse (2021), comparing each pixel’s SO in a given year to its multi-year mean. However, due to missing SO estimates for some pixels in certain years – caused by data gaps exceeding the interpolation window – and the overall short time series, we chose the



fixed-threshold approach. Analysis of long-term ICP Forests observations indicates that early senescence occurs episodically rather than systematically at specific sites (Figure S4), supporting the use of a fixed threshold to identify early senescence events as deviations from normal phenological timing.

SO maps at 10 m resolution were used to quantify the forest area affected by early senescence for each species and year. The overall analysed forest area was 22,462 km<sup>2</sup> for beech and 12,537 km<sup>2</sup> for oak. For subsequent analyses involving climate and soil variables, we aggregated the 10 m SO maps to 1 km resolution to match the spatial resolution of these covariates. This was done by averaging the SO values of beech- or oak-dominated forest pixels within each 1×1 km grid cell. To ensure representativeness and signal quality, we only computed species-specific averages for cells in which the respective forest type (beech or oak) covered ≥10% of the area, thereby limiting the influence of isolated and potentially noisy pixels. This criterion retained on average 82.2% (18,466 km<sup>2</sup>) of the total beech forest area, and 60.6% (7,602 km<sup>2</sup>) of the total oak forest area. This subset of pixels still spans the main environmental gradients across Germany and provides a sufficient sample size (n=65,548 for beech, n=36,843 for oak) for robust statistical inference. Figure S5 visualizes the distribution of the number of species-specific 10 m pixels within these upscaled 1 km pixels. SO<sub>early</sub> at the 1 km scale was defined based on the aggregated mean DoY before 244.

## 2.2 Atmospheric and soil drought data

We calculated hourly vapor pressure deficit (VPD) for April–August from 2018–2023 using the German Weather Service’s gridded HOSTRADA dataset, which provides near-surface air and dew point temperatures at 1 km resolution based on interpolated station data (DWD, 2024). We extracted daily maximum VPD values (VPD<sub>max</sub>), which typically occur in the early afternoon and are more indicative of drought stress experienced by plants than daily means, because stomatal regulation and hydraulic stress responses are strongest under the highest VPD conditions of the day (Grossiord et al., 2020). Soil water potential ( $\psi_{\text{soil}}$ ) under beech and oak forests for 2018–2023 was also obtained from the German Weather Service as 8-day averages at 1 km resolution (P. Schmidt-Walter, personal communication, April 2025). This data was generated with the hydrological model LWF-Brook90 (Hammel & Kennel, 2001; Schmidt-Walter et al., 2020). LWF-Brook90 estimates soil water potential and moisture dynamics within the species-specific rooting (1.4 m for beech, 1.8 m for oak) using parameters based on Schmidt-Walter et al. (2019) and Weis et al. (2023).

## 2.3 Statistical modelling of senescence responses

We used logistic regression to assess the influence of atmospheric and soil drought stress on senescence onset, treating the outcome as binary variable: 0 for SO<sub>normal</sub> and 1 for SO<sub>early</sub>. This approach was chosen for its simplicity, robustness, and ability to estimate probabilities of early senescence while providing interpretable coefficients. All models were run separately for beech and oak forests using data from all years.



### 160 **2.3.1 Univariate models**

First, we fitted univariate models using either  $VPD_{max}$  or  $\psi_{soil}$  as predictors. As we assumed that  $SO_{early}$  occurs after a period of cumulative drought stress, we evaluated multiple averaging periods for both  $VPD_{max}$  and  $\psi_{soil}$ . These periods extended from mid- to late August (the month with highest frequency of  $SO_{early}$ ) in biweekly time steps back to 1 April, the approximate start of the growing season. We selected the optimal averaging period for each predictor based on the highest

165 F1-score (harmonic mean of precision and recall) from logistic regression models using 5-fold cross-validation with random splits. To address class imbalance resulting from a substantially lower number of occurrences of  $SO_{early}$  (~13%) compared to  $SO_{normal}$  (~87%), we applied weighting by inverse class frequencies during model fitting. Thresholds for drought stress triggering early senescence were derived from the logistic regression probability scores, with the 50% probability level defining the threshold.

### 170 **2.3.2 Bivariate models**

We fitted bivariate models using both  $VPD_{max}$  and  $\psi_{soil}$  as predictors to assess the relative contributions of atmospheric and soil drought stress to  $SO_{early}$ . Prior to modelling, predictors were standardized to zero mean and unit variance to allow direct comparison of effect sizes. The coefficients were derived across five random cross-validation splits and represent the change in the log-odds ( $\log(p/(1-p))$ ), with  $p$ =probability of  $SO_{early}$  of  $SO_{early}$  per standard deviation increase in the predictor.

175 Positive coefficients indicate that the likelihood of early senescence increases with the predictor, while absolute values reflect the contribution of each predictor to  $SO_{early}$ .

We also explored bivariate models combining the most predictive averaging periods from summer and spring to evaluate the relative influence of drought at different seasonal stages. Interaction terms between predictors were tested for all bivariate models, but were retained only when they improved model performance (F1-score). To account for potential site-specific

180 adaptation of trees to local conditions, we additionally tested models using standardized anomalies (z-scores) for both  $VPD_{max}$  and  $\psi_{soil}$  for the respective averaging periods, computed based on data for 2010–2023.

### **2.4 Senescence–mortality relationships**

To assess the relationship between early leaf senescence and subsequent canopy mortality, we used the cover fraction of standing deadwood in the tree canopy for Germany from 2018–2021 (Schiefer et al., 2025) derived from high-resolution

185 UAV imagery combined with Sentinel-1 and Sentinel-2 data. Since our focus was on increases in canopy mortality following early leaf senescence, we calculated year-to-year differences in deadwood cover and retained only positive changes. Negative changes could be related to both removal of dying trees or canopy regrowth and were thus neglected. We then aggregated the mortality increase maps to 1 km resolution by averaging across pixels within the respective forest types. We compared the distributions of mortality increase for forest pixels having experienced normal, early (for this analysis defined

190 as  $SO$  between 15–31 August) or very early senescence (before 15 August) in the preceding year. Differences in median



mortality increases between these groups were assessed using two-sided Mann–Whitney U tests. To evaluate the effect of repeated early senescence events on canopy mortality, we also compared forest pixels with no, single, or multiple occurrences of early leaf senescence in preceding years.

## 2.5 Drought vulnerability classification

195 Based on the previous analyses, we classified beech and oak forest pixels into different drought response types according to senescence timing, drought sensitivity, and mortality patterns. We therefore applied K-means clustering to eight variables: mean SO, SO variability, SO<sub>early</sub> frequency, next-year mortality increase, and correlations of SO with VPD<sub>max</sub> and  $\psi_{\text{soil}}$  in spring and summer. These variables describe whether a forest pixel tends to senesce earlier or later, its interannual variability, responsiveness to atmospheric and soil drought stress, and vulnerability to drought-induced damage. The optimal  
200 number of clusters ( $k=3$ ) was selected based on the inertia criterion (within-cluster sum of squares) while maintaining interpretability. To characterize and interpret the identified drought response types, we examined their associations with a range of stand, climatic, and edaphic variables. These included canopy cover, height, and height variability (as proxies for stand structure); leaf maturation date (VI reaches 80% of the annual amplitude in spring); seasonal and annual averages (calculated across all years) of temperature, climatic water balance (CWB), VPD,  $\psi_{\text{soil}}$  at multiple depths (0–50, 0–100, 0–  
205 150 cm) and relative extractable water (REW) in the root zone; soil depth, texture (sand, silt, clay fractions), and bulk density; and topography (elevation, slope, exposition). All datasets were harmonized to 1 km resolution by upscaling higher-resolution datasets using spatial averaging, and stand metrics were computed separately for beech- and oak-dominated forests. Data sources are listed in Table S2. To reduce redundancy and focus on the most informative variables, highly correlated environmental variables were grouped via hierarchical clustering, and only the variable with the highest mutual  
210 information with the drought response types was retained from each group.

## 3 Results

### 3.1 Early senescence during the 2018–2023 period

Satellite observations revealed widespread occurrences of early leaf senescence across Germany’s deciduous forests during the recent drought sequence (Figure 1). Early senescence affected 42.9 % of the analysed forest area in 2018, and remained  
215 substantial in 2019 (22.8 %) and 2022 (20.1 %), while it was less common in 2020 and 2021, and rare in 2023. Spatial patterns of early senescence varied among years, with the most extensive signals in 2018 occurring across large parts of central Germany, and shifting regional hotspots in subsequent years – including north-eastern regions in 2019, central-western regions in 2020, and more spatially fragmented occurrences in 2022. While the absolute area affected was consistently larger in beech forests (2018: 8,769 km<sup>2</sup>) than in oak (2018: 5,048 km<sup>2</sup>), both forest types were affected in  
220 similar proportions each year, indicating that drought exposure drove canopy stress broadly across species. Across the full study period, both forest types showed similar cumulative exposure and recurrence patterns: approximately 38.6% of forests



never experienced early senescence, while 31.4% were affected once, 18.2% twice, and 11.8% three or more times, corresponding to 61.4% of forest area affected at least once. These patterns demonstrate that early senescence was a widespread and recurrent response to drought across Central European deciduous forests during the 2018–2023 period. To understand the environmental conditions underlying this response, we next quantified the cumulative atmospheric and soil drought conditions associated with its occurrence.

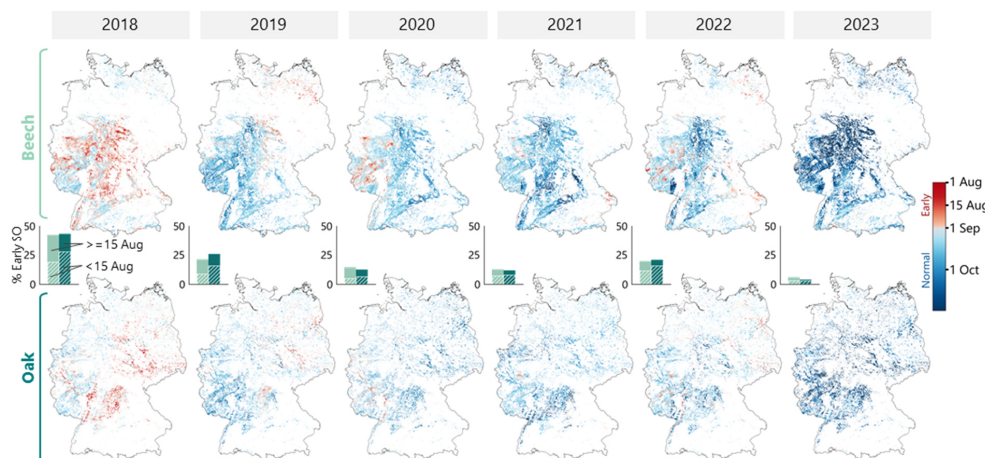


**Figure 1:** Spatial patterns of senescence onset (SO) in beech- and oak-dominated forests across Germany (2018–2023) at 1 km resolution. Colors represent the mean SO of all species-specific 10 m pixels within each grid cell. Red indicates early senescence onset ( $SO_{early}$ ), defined as occurring before day-of-year 244, i.e., 1 September in non-leap years. Bar plots show the proportion of forest area exhibiting  $SO_{early}$  for beech (light green) and oak (dark green). Hatched bars distinguish very early senescence (before 15 August) from later  $SO_{early}$  events.

### 3.2 Cumulative drought stress triggers early senescence

Early leaf senescence ( $SO_{early}$ ) was associated with cumulative atmospheric and soil drought conditions – captured by daily maximum atmospheric vapour pressure deficit ( $VPD_{max}$ ) and root-zone soil water potential ( $\psi_{soil}$ ) – in both forest types. To identify the drought integration windows most predictive of  $SO_{early}$ , we evaluated logistic regression models across different candidate time periods (Figure 2a-b, Table S3). The most predictive atmospheric drought window was the six-week period from early July to mid-August, whereas the soil drought window was shorter and covered the second half of August.

The probability of  $SO_{early}$  increased sharply once drought stress in the identified time periods exceeded species-specific thresholds (Figure 2c-d). For beech forests, the 50% probability threshold was crossed when  $VPD_{max,summer}$  exceeded 1.89 kPa over the six-week period (1 July–15 August) or when  $\psi_{soil,summer}$  dropped below -0.81 MPa in the following two-week period (15–30 August). In oak forests, the corresponding thresholds occurred at a  $VPD_{max,summer}$  of 2.06 kPa and a  $\psi_{soil,summer}$



of  $-0.93$  MPa. Although model performance was moderate ( $F1 \approx 0.55$ – $0.57$ ), predictive skill substantially exceeded that of a random baseline, indicating that cumulative drought conditions capture the dominant drivers of early senescence at landscape scale despite local variability in stand characteristics and site conditions.

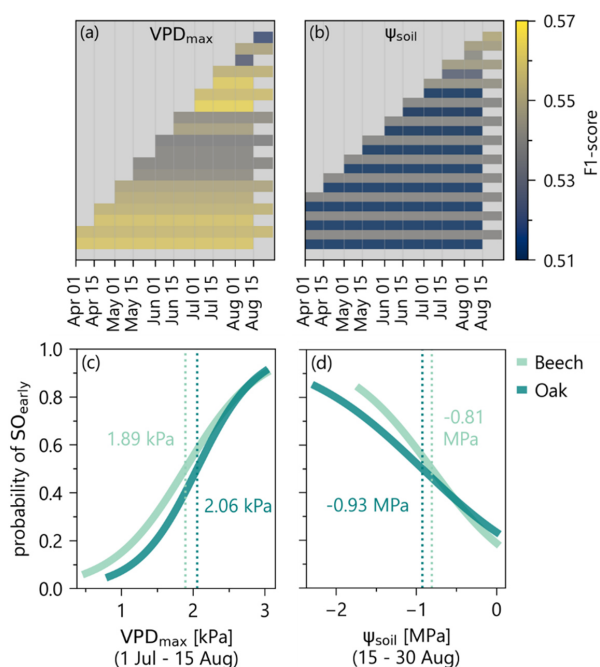


**Figure 2:** Atmospheric and soil drought effects on early leaf senescence ( $SO_{early}$ ). a-b) Performance (F1-score) of univariate logistic regression models predicting  $SO_{early}$  across candidate accumulation periods for atmospheric ( $VPD_{max}$ ) and soil drought ( $\psi_{soil}$ ). c-d) Modelled probability of  $SO_{early}$  for the most predictive accumulation periods (1 Jul–15 Aug for  $VPD_{max}$ ; 15–30 Aug for  $\psi_{soil}$ ) in beech and oak. Vertical dotted lines indicate species-specific threshold values at which the predicted probability of  $SO_{early}$  reaches 50%. Root-zone soil water potential ( $\psi_{soil}$ ) was integrated over 1.4 m for beech and 1.8 m for oak forests.

### 3.3 Species-specific drought sensitivities

The relative importance of atmospheric and soil drought differed between species. Bivariate logistic regression models revealed that in beech forests,  $SO_{early}$  was more strongly associated with declining soil water potential ( $\psi_{soil,summer}$ ), whereas atmospheric drought ( $VPD_{max,summer}$ ) exerted a stronger influence in oak forests (Figure 3a). Distributions of  $\psi_{soil,summer}$  support this pattern, showing a clearer separation between early and normal senescing forests in beech than in oak, despite



generally lower  $\psi_{\text{soil,summer}}$  in oak (Figure 3g). Meanwhile,  $\text{VPD}_{\text{max,summer}}$  reveals stronger atmospheric dryness in early  
 260 senescing oak forests compared to beech (Figure 3e).

Including spring drought conditions in the models indicated that  $\text{SO}_{\text{early}}$  was driven by drought stress accumulating across  
 multiple seasonal stages. The most predictive spring windows were – similar to the summer periods – six weeks for  
 $\text{VPD}_{\text{max,spring}}$  (15 Apr–30 May), and two weeks for  $\psi_{\text{soil,spring}}$  (15–30 May) (Table S4). In particular, elevated atmospheric  
 demand during spring increased the likelihood of  $\text{SO}_{\text{early}}$  later in the growing season (Figure 3b, f), while early-season soil  
 265 water potential was still near-zero and contributed little to predicting  $\text{SO}_{\text{early}}$  (Figure 3c, h). Models combining spring  
 $\text{VPD}_{\text{max,spring}}$  with  $\psi_{\text{soil,summer}}$  showed that beech remained more sensitive to summer soil drought, while oak showed stronger  
 responses to spring atmospheric drought (Figure 3d). Analyses that used standardised anomalies of the drought indicators as  
 predictors showed similar patterns, but generally increased the importance of  $\psi_{\text{soil,summer}}$  for both species (Figure S6).  
 Overall, early senescence reflects a cumulative drought sequence, in which elevated spring VPD increases the likelihood of  
 270 occurrence and summer soil water deficits act as critical thresholds. This response is species-specific, with beech primarily  
 limited by soil water availability and oak by atmospheric demand.

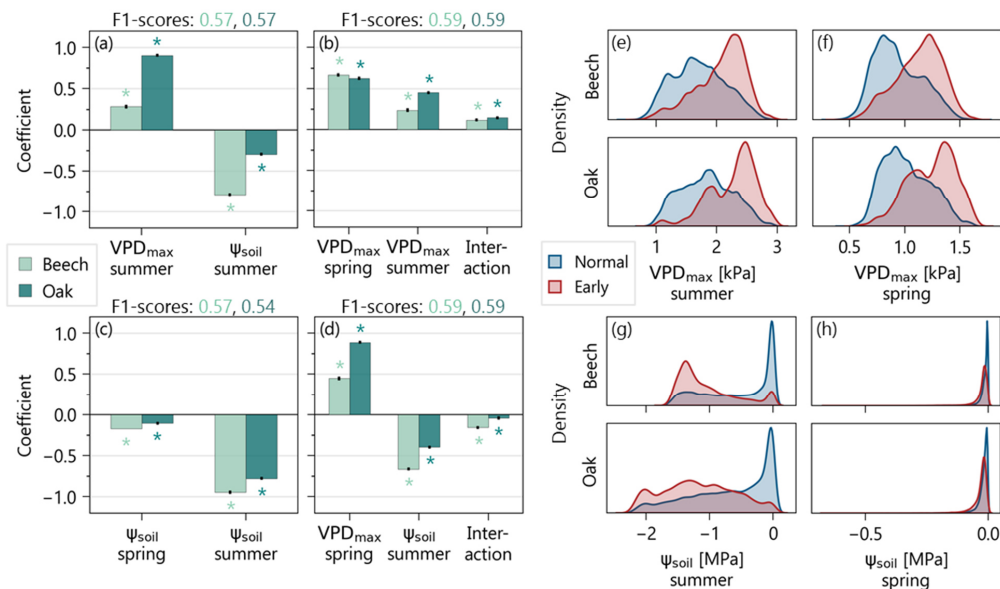


**Figure 3:** Species-specific effects of atmospheric and soil drought on early leaf senescence ( $\text{SO}_{\text{early}}$ ). a-d) Standardised regression  
 275 coefficients (effect sizes) from bivariate logistic regression models including combinations of atmospheric ( $\text{VPD}_{\text{max}}$ ) and soil drought  
 ( $\psi_{\text{soil}}$ ) during spring and summer. Black error bars indicate standard deviations of the coefficients across five cross-validation folds.  
 Asterisks denote statistically significant coefficients. e-h) Probability density distributions of summer and spring  $\text{VPD}_{\text{max}}$  (e-f) and  $\psi_{\text{soil}}$  (g-  
 h) for normal (blue) and early senescing (red) forest pixels in beech (top) and oak (bottom).



### 3.4 Early senescence is associated with canopy mortality

To assess whether early senescence reflects progressive physiological damage or a protective drought-avoidance response, we examined canopy mortality in the year following early senescence events. Forest pixels experiencing early leaf senescence consistently showed significantly higher increases in canopy mortality in the following year compared with forests exhibiting normal senescence timing ( $p < 0.05$ ). This relationship held for both species and all years, with the exception of beech mortality in 2020 following early senescence in 2019 (Figure 4a-c). The strongest increases in mortality – expressed as percentage cover of the respective forest pixel – were observed following very early senescence events, defined here as occurring before 15 August. Mortality increased by up to 5.8 percentage points (pp) in beech and 7.9 pp in oak in 2019 after very early senescence in 2018 compared to 3.9 pp and 5.5 pp in normal senescing forests, respectively, indicating that exceptionally early canopy decline reflects severe physiological stress. Mortality risk was further elevated in stands experiencing repeated early senescence across multiple years ( $p < 0.05$ ) (Figure 4d-e). Three consecutive early senescence events across 2018–2020 increased mortality in 2021 by up to 6.2 pp in beech and 6.8 pp in oak compared to 4.4 pp and 5.0 pp in forests with only one event, suggesting cumulative damage from recurrent drought stress. Together, these results indicate that early senescence serves as a landscape-scale indicator of declining forest vitality and emerging mortality risk.

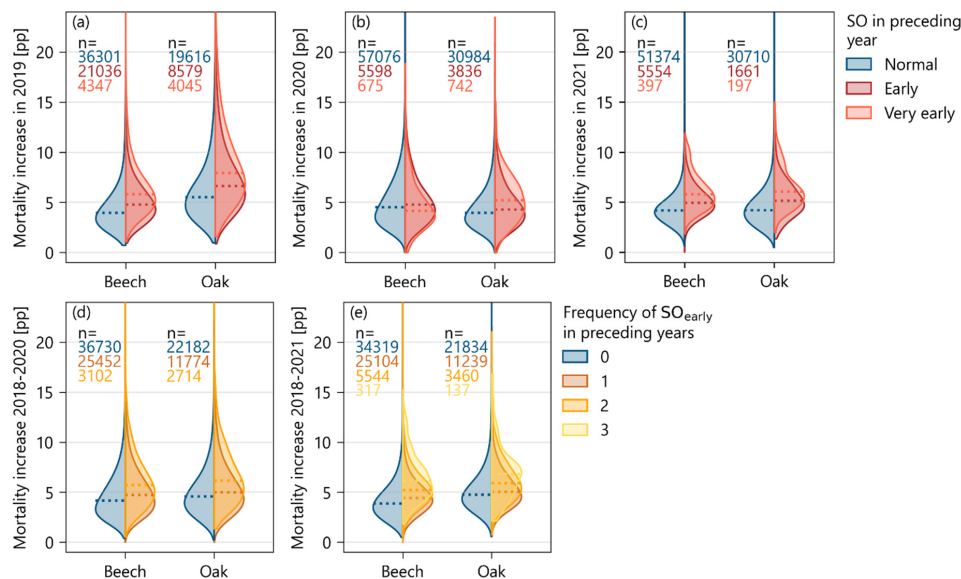


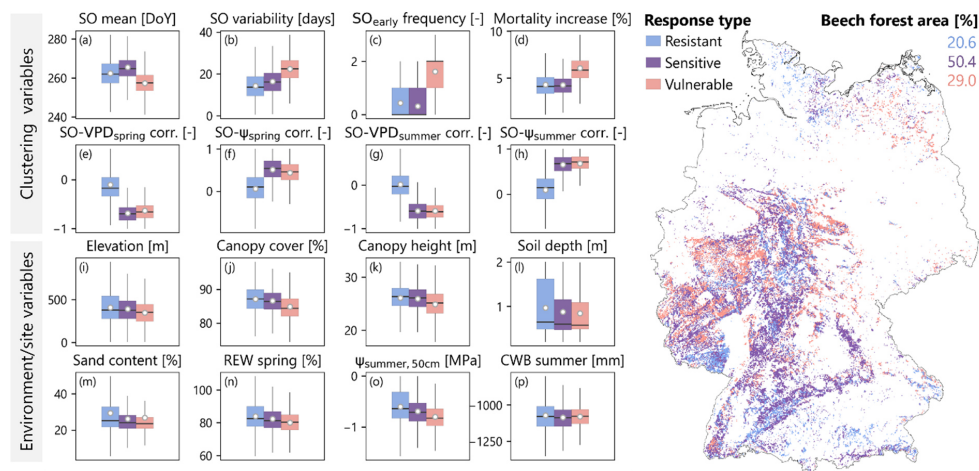
**Figure 4:** Canopy mortality following early leaf senescence in beech and oak forests in Germany. a-c) Pixel-level increases in next-year canopy mortality (percentage points) for forest with normal, early, or very early (before 15 August) senescence in the preceding year, based on data from Schiefer et al. (2023). Mortality data are available for 2018–2021; therefore, analyses link senescence in 2018–2020 to mortality in the following year. Numbers indicate sample sizes, and horizontal dotted lines show medians. Longer-term mortality effects



are shown in Figure S7. d-e) Increases in canopy mortality in 2020 and 2021 (relative to 2018) depending on the frequency of early senescence events in preceding years. Y-axes are truncated to improve visibility; full distributions are shown in Figure S8.

### 3.5 Spatial patterns of forest drought vulnerability

300 Clustering forest pixels based on senescence dynamics, drought sensitivity, and mortality patterns across the 2018–2023 study period revealed three distinct drought-response types across Germany’s deciduous forests (Figure 5-6). The proportional distribution of response types was highly consistent across beech and oak – resistant (beech: 20.6%, oak: 18.2%), sensitive (beech: 50.4%, oak: 51.1%), and vulnerable (beech: 29.0%, oak: 30.7%) – indicating that these response types primarily reflect landscape-level environmental gradients rather than species-specific traits.



305

**Figure 5:** Clustering of beech forest pixels based on senescence dynamics, drought sensitivity, and mortality patterns. Eight variables (a-h) were used to classify three drought-response types: resistant (blue), sensitive (violet), and vulnerable (pink). Resistant forests show low drought sensitivity of senescence timing (e-h) and low  $SO_{early}$  frequency (c), sensitive forests show high drought sensitivity but low  $SO_{early}$  frequency; vulnerable forests show high drought sensitivity, frequent  $SO_{early}$ , and increased mortality. Boxplots (i-p) illustrate differences in environmental and site variables across response types. Variables were selected based on hierarchical clustering and mutual information with the response types. REW: relative extractable water; CWB: climatic water balance. The map shows the spatial distribution of drought-response types across Germany’s beech forests.

310

Resistant forests showed limited sensitivity of senescence timing to drought conditions – indicated by near-zero correlations of spring and summer  $VPD_{max}$  and  $\psi_{soil}$  with senescence onset – and rarely experienced early senescence during the study period. Post-hoc characterisation of these clusters revealed that resistant forests were predominantly located in regions with comparatively favourable moisture conditions, including higher-elevation areas and regions with greater precipitation. Stands were characterised by taller and closed canopies, later spring phenology, deeper soils, and greater water availability –

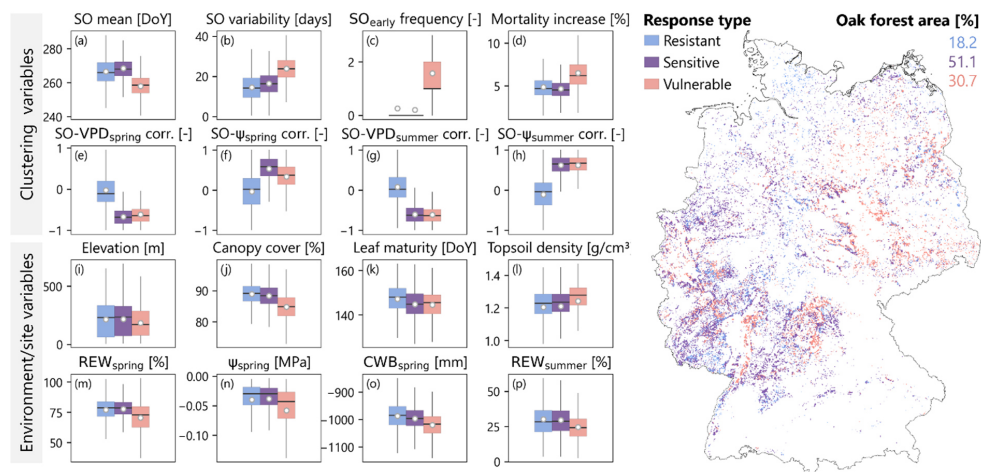
315



320 conditions that buffer trees against severe drought. Correspondingly, these forests exhibited the lowest increases in canopy mortality following drought years.

Sensitive forests represented an intermediate response type, showing clear drought-related shifts in senescence timing but still infrequent early senescence events. They were widely distributed across Germany and typically occurred in regions with moderate precipitation and intermediate soil water storage capacity. In these stands, senescence responded to both atmospheric and soil drought, indicating that drought effects emerge once local buffering capacity is exceeded, but rarely become severe enough to trigger widespread canopy decline.

325 Vulnerable forests exhibited strong drought responses, including frequent early senescence events and the largest increases in canopy mortality following drought years. These stands were concentrated primarily in lowland regions characterised by comparatively drier climatic conditions, more open canopies, and shallower, more compacted soils with limited water availability. Senescence timing of these stands was strongly controlled by both  $VPD_{max}$  and  $\psi_{soil}$ , indicating high sensitivity and exposure to drought stress. Overall, these response types reveal pronounced spatial variability in drought vulnerability across temperate forests, driven by the interaction of local climate, soil, and stand structure.



335 **Figure 6:** Clustering of oak forest pixels based on senescence dynamics, drought sensitivity, and mortality patterns, analogous to Figure 5. Three drought-response types are identified: resistant (blue), sensitive (violet), and vulnerable (pink). Boxplots (a–p) show differences in clustering variables and environmental and site characteristics across response types. Variables were selected based on hierarchical clustering and mutual information with the response types. The map shows the spatial distribution of drought-response types across Germany’s oak forests.



#### 4 Discussion

##### 340 4.1 Early senescence tracks drought impacts across the 2018–2023 period

Our remotely sensed senescence maps revealed that the majority of the deciduous forest area in Germany showed premature canopy decline during the study period. While the satellite-observed patterns showed pronounced spatial and temporal variability, they closely mirror independent reports of observed drought impacts reported across Germany during 2018–2023, supporting their validity as indicators of forest drought stress. The most extensive signal in 2018, when large  
345 contiguous areas across central Germany exhibited early senescence, is consistent with widespread reports of leaf curling, premature coloration, and even green leaf abscission from different forestry institutions (FVA-BW, 2018; NW-FVA, 2018; SBS, 2018; TMIL, 2018). Geographic hotspots shifted in subsequent years, tracking regional reports of deteriorating crown condition and rising crown dieback, often accompanied by increased insect and pathogen activity in drought-weakened stands (LFE, 2019; LM, 2019; NW-FVA, 2019; TMIL, 2020). This suggests that detections in these years reflect not only  
350 immediate drought responses but also progressive vitality decline in chronically stressed stands, consistent with the lagged mortality effects we document. Particularly in 2022, early senescence re-emerged in previously affected regions, highlighting stands that repeatedly experienced severe drought stress (FAWF, 2022; FVA-BW, 2022; LFE, 2022; LM, 2022). Lower prevalence of early senescence in 2021 and 2023 shows that satellite-observed patterns also reflect the reduction in acute drought stress symptoms and partial canopy recovery during wetter and cooler years (FVA-BW, 2023;  
355 LM, 2023; NW-FVA, 2021; Wald und Holz NRW, 2021). Overall, these patterns underscore the value of annual, spatially continuous senescence mapping for tracking both immediate physiological stress and cumulative forest decline across drought years.

The remarkably similar cumulative and recurrence patterns across beech and oak point to shared landscape-scale controls on drought stress exposure during this period. This convergence is notable given the well-documented physiological differences  
360 between the two species, e.g. in rooting patterns and stomatal regulation (Klein, 2014; Leuschner et al., 2001; Pietig et al., 2026), and suggests that the severity and spatial extent of the 2018–2023 drought sequence was sufficient to override species-level differences in vulnerability at the landscape scale. However, despite similar exposure patterns, our analysis revealed non-identical responses across both species: beech and oak showed distinct sensitivities to soil and atmospheric drought, and differed to some extent in their drought thresholds, indicating that convergent outcomes may emerge from  
365 divergent physiological pathways.

##### 4.2 Early senescence reflects hydraulic thresholds

Early leaf senescence in temperate deciduous forests emerged once cumulative atmospheric and soil drought thresholds were exceeded. Across Germany's beech and oak forests, the probability of early senescence increased sharply after root-zone soil water potential ( $\psi_{\text{soil}}$ ) declined below approximately  $-0.8$  MPa in beech and  $-0.9$  MPa in oak, following sustained periods of  
370 elevated atmospheric vapour pressure deficit (VPD). These thresholds reflect the accumulation of hydraulic stress over



several weeks rather than a response to short drought events. The most predictive time windows – six weeks for  $VPD_{max}$  followed by two weeks for  $\psi_{soil}$  – capture complementary stages of hydraulic stress accumulation: sustained atmospheric demand progressively depletes soil water reserves until tree water status approaches critical levels (cf. Grossiord et al., 2020), and together these processes provide strong predictive power for early senescence occurrence.

- 375 The hydraulic threshold identified for beech in this study closely aligns with the -0.8 MPa root-zone  $\psi_{soil}$  threshold for the onset of defoliation and embolism formation previously identified by Walthert et al. (2021) from plot-scale field observations in Swiss beech forests. This convergence of findings between our satellite-based landscape-scale analysis and independent field measurements supports the broader generality of the identified threshold across a range of site conditions in Central Europe. For oak, the more negative threshold of -0.93 MPa, together with a deeper simulated rooting zone (1.8 m  
380 in oak vs. 1.4 m for beech), reflects higher drought resistance and the capacity to sustain water transport under drier conditions (Bréda et al., 2006; Cochard et al., 1992). Nevertheless, this thresholds remains above the pre-dawn leaf water potential of approximately -1.3 MPa at which symptoms of leaf injury in temperate oaks increase under experimental conditions (Günthardt-Goerg et al., 2013), highlighting the importance of deep soil water access in natural stands, where a root-zone integrated  $\psi_{soil}$  of -0.93 MPa may already reflect substantial depletion.
- 385 The detection of distinct species-specific drought thresholds for canopy senescence highlights that remote sensing observations can reveal physiologically meaningful stress limits that are consistent at the landscape scale. Identifying such thresholds is critical for improving ecosystem models to better represent drought impacts on forest productivity, phenology, and vitality, thereby enabling more accurate predictions of forest responses to climate extremes,

#### 4.3 Species-specific sensitivities to atmospheric and soil drought

- 390 Both soil and atmospheric drought acted as cumulative drivers of early leaf senescence, but their relative strength differed between species. We found beech to be more sensitive to soil water deficits, consistent with its shallower rooting system, relatively isohydric stomatal strategy, and well-documented dependence on surface soil water reserves (Gessler et al., 2022; Jonard et al., 2011; Leuzinger et al., 2005). As soil water potential declines, beech becomes increasingly vulnerable to embolism formation and hydraulic dysfunction, which has been linked to premature leaf senescence in beech during the  
395 2018 drought (Schuldt et al., 2020; Walthert et al., 2021).

- In contrast, early senescence in oak was more closely associated with atmospheric drought. This likely reflects reduced restriction by soil moisture due to deeper root uptake and greater resistance to drought-induced cavitation, which allows oaks to maintain hydraulic function under more negative soil water potentials (Leuschner & Meier, 2018; Scharnweber et al., 2013). However, the higher hydraulic conductance and transpiration rates of oaks may also contribute to a greater hydraulic  
400 risk under sustained high atmospheric demand (Manzoni et al., 2013), potentially explaining the stronger influence of VPD on senescence probability. It should be noted that stomatal behaviour differs between the two investigated oak species: stronger stomatal regulation in response to drought has been reported for *Q. robur* (Niemczyk et al., 2024) but not for *Q. petraea* (Backes & Leuschner, 2000), and our landscape-scale results likely integrate across both species. Beyond direct



hydraulic effects, oak's sensitivity to atmospheric drought may additionally reflect indirect biotic pathways: warm and dry  
405 conditions increase the likelihood of insect outbreaks (Haynes et al., 2022; Karolewski et al., 2007), which can compound  
hydraulic stress and accelerate canopy decline independently of soil water deficits (Gosling et al., 2024; Rodríguez-  
Calcerrada et al., 2017).

#### 4.4 Role of early-season drought

Elevated spring atmospheric dryness further amplified early senescence risk in both species. While such legacy effects have  
410 been reported previously (Bigler & Vitasse, 2021; Fu et al., 2014; Zuccarini et al., 2023), the underlying mechanisms remain  
uncertain. Proposed pathways include earlier leaf-out accelerating soil water depletion and advancing the onset of critical  
soil water deficits (Bigler & Vitasse, 2021), cumulative stress constraining the functional leaf lifespan following early  
budburst (Mariën et al., 2021; Zuccarini et al., 2023), and sink limitation, where high early-season productivity triggers  
earlier senescence via carbon storage feedbacks (Fu et al., 2014; Zani et al., 2020).

415 Our data show that spring VPD is a stronger predictor than spring soil water potential, suggesting that the seasonal legacy  
effect operates primarily through early atmospheric stress on leaf and hydraulic function rather than through accelerated soil  
water depletion alone. Consistent with this, dry springs limit the formation of new sapwood needed to sustain transpiration of  
the fully developed leaf area, thereby increasing hydraulic vulnerability later in the season (Alongi et al., 2025; Bose et al.,  
2021; Etzold et al., 2022). Oak appears particularly susceptible to this mechanism, as water transport in this ring-porous  
420 species relies on newly formed earlywood and oak growth responses are known to be strongly sensitive to spring conditions  
(Bose et al., 2021; Vanhellemont et al., 2019), potentially explaining the high sensitivity of early senescence to spring  
VPD<sub>max</sub>. Particularly in 2019 and 2020, early season drought resulted in strong radial growth reductions (Scharnweber et al.,  
2020; Thom et al., 2023), likely constraining water transport and contributing to early leaf senescence in these years.  
Overall, combined spring and summer droughts, events expected to become more frequent across Europe (Spinoni et al.,  
425 2018), may amplify canopy stress through cumulative seasonal legacy effects.

#### 4.5 Early senescence as an early warning signal of forest decline

Our results show that exceptionally early and recurrent early senescence are associated with increased canopy mortality in  
subsequent years, indicating that early senescence reflects drought-induced vitality decline (Frei et al., 2022) rather than  
transient acclimation. While satellite-based mortality estimates may potentially not fully distinguish mortality from  
430 defoliation, the observed patterns align with independent physiological evidence. In beech, early senescing trees often show  
persisting embolisms and reduced secondary growth, limiting their ability to restore hydraulic function and predisposing  
them to canopy dieback in subsequent years (Arend et al., 2022; Braun et al., 2021; Neycken et al., 2024; Schuldt et al.,  
2020). In oak, persisting xylem embolisms are less likely to cause mortality because hydraulic function depends on the  
newly formed xylem each year, but repeated early senescence and drought may deplete carbon reserves, which are required  
435 in large quantities to form sufficient functional earlywood in the next season (Plotkin et al., 2021). Under severe drought,



additional carbon allocation to replace drought-killed fine roots (Leonova et al., 2022) may further exacerbate reserve depletion. Elevated oak mortality has also been reported when drought coincides with repeated insect defoliation, emphasizing the importance of drought–insect interactions for canopy decline (Tanzer et al., 2025). The overall modest increases in canopy mortality and the absence of significantly elevated mortality following early senescence in beech in 2019 suggest that not all early senescence events reflect severe or lasting damage, and that mortality outcomes likely depend on drought severity, recurrence, recovery capacity, and interacting stressors. Nevertheless, with the single exception of beech in 2019, early senescence was consistently associated with elevated mortality, supporting the interpretation that early senescence more often reflects stress-induced damage than effective drought avoidance. Therefore, early senescence serves as a physiological early-warning signal for emerging mortality risk and enables targeted monitoring of drought-induced forest decline.

#### 4.6 Spatial patterns of drought vulnerability

Our study revealed pronounced spatial variation in drought-induced leaf senescence and mortality across Germany's forests. This heterogeneity in drought vulnerability was primarily controlled by local soil water availability, a pattern that is consistent across scales: site-level studies link higher growth sensitivity to climate variability and more severe crown damage to soils with lower water storage capacity (Klesse et al., 2022), while global analyses show greater drought sensitivity of leaf senescence in more arid regions (Li et al., 2025). Drought sensitivity of both beech and oak forests declined at higher elevations, where lower temperatures and higher precipitation reduce drought exposure, consistent with previous observations of delayed senescence under such conditions (Bigler & Vitasse, 2021; Lukasová et al., 2020). Conversely, forests in lowland areas showed higher vulnerability, particularly on shallower and drier soils with less favourable growing conditions (Klesse et al., 2022; Walthert et al., 2021). We further found increased drought vulnerability of beech on sites with low sand content, while oak was more vulnerable on soils with higher bulk density. This aligns with reports of increased drought damage on loamy, compacted soils that become cemented during prolonged drought and impair fine root growth and function (LFE, 2019; SBS, 2018). Stand structure further modulated drought responses. We detected greater drought sensitivity of leaf senescence in more open stands, where increased solar radiation and evaporative demand likely accelerate leaf ageing and canopy dehydration. Observations of early leaf coloration along forest edges and in single exposed trees support this interpretation (FVA-BW, 2018; LFE, 2019; Wohlgemuth et al., 2020) and highlight the role of microclimatic buffering within closed forest canopies (De Frenne et al., 2021).

In summary, drought vulnerability arises from the interaction of regional climate exposure and local site properties that regulate water availability and microclimate, demonstrating the value of satellite-observed early senescence as a spatially resolved indicator of forest drought stress. The spatial vulnerability framework identifies forests and site conditions most prone to exceeding drought stress thresholds and provides a basis for targeting adaptive management, which may include species composition adjustment toward more drought-tolerant mixtures on vulnerable sites and maintenance of canopy closure.



### Conclusions

470 This study establishes satellite-observed early leaf senescence as a spatially explicit indicator of cumulative drought stress and vitality decline across temperate beech- and oak-dominated forests. The consistent link between early senescence and subsequent mortality confirms that premature leaf shedding reflects physiological damage rather than protective adjustment, while the species-specific hydraulic thresholds and sensitivity patterns identified here provide a mechanistic basis for interpreting remote sensing signals of canopy stress and for improving the representation of drought-driven senescence dynamics in ecosystem models — with direct implications for projections of carbon cycling and forest mortality under future climate extremes. The spatially explicit vulnerability framework further reveals that drought responses are strongly modulated by local site conditions, identifying the forests most at risk of transitioning from stress to irreversible decline. Together, these findings offer a near-real-time, landscape-scale tool for tracking emerging drought risk, anticipating mortality hotspots, and targeting management interventions to sustain forest resilience across temperate regions.

### 480 Data availability

The data supporting the findings of this study will be openly available in the RADAR4KIT repository (<https://radar.kit.edu/radar/en/home>) and assigned a persistent DOI.

### Author contributions

PL contributed to conceptualization, methodology, validation, formal analysis, visualization, writing of the original draft. 485 AB and NKR contributed to conceptualization, methodology, reviewing and editing of the manuscript draft. RG and MT contributed to reviewing and editing of the manuscript draft. NKR acquired the funding supporting this study.

### Competing interests

The authors declare that they have no competing interests associated with this manuscript.

### Acknowledgements

490 We thank Paul Schmidt-Walther (DWD) for providing soil water potential and relative extractable water data from LWF-Brook90. Evaluation of satellite-derived senescence onset was based on data collected by partners of the official UNECE ICP Forests Network (<http://icp-forests.net/contributors>). Part of the data was co-financed by the European Commission (Data accessed on 22/01/2025). We thank Tanja Sanders for her assistance with acquisition of the ICP Forests data and helpful comments on related aspects of the manuscript. Satellite data processing was performed on the EO-Lab platform,



495 operated by DLR and funded by the German Federal Ministry for Economic Affairs and Climate Action (BMWK). We used  
ChatGPT (OpenAI) to assist with code development and Claude (Anthropic) improve the readability and logical flow of the  
manuscript text. All AI-assisted content was reviewed, edited by the authors, who take full responsibility for the final  
content.

### Financial support

500 This study was funded through the Helmholtz Initiative and Networking fund (W2/W3-156).

### References

- Alongi, F., Knüver, T., McAdam, S. A. M., Ziegler, Y., Gast, A., & Ruehr, N. K. (2025). Drought-induced delays in stem  
hydraulic development shape gas exchange and growth recovery in Douglas fir. *Plant Physiology*, kiaf654.  
<https://doi.org/10.1093/plphys/kiaf654>
- 505 Arend, M., Link, R. M., Zahnd, C., Hoch, G., Schuldt, B., & Kahmen, A. (2022). Lack of hydraulic recovery as a cause of  
post-drought foliage reduction and canopy decline in European beech. *New Phytologist*, 234(4), 1195–1205.  
<https://doi.org/10.1111/nph.18065>
- Backes, K., & Leuschner, C. (2000). Leaf water relations of competitive *Fagus sylvatica* and *Quercus petraea* trees during 4  
years differing in soil drought. *Canadian Journal of Forest Research*, 30(3), 335–346. <https://doi.org/10.1139/x99->  
510 205
- Bevacqua, E., Rakovec, O., Schumacher, D. L., Kumar, R., Thober, S., Samaniego, L., Seneviratne, S. I., & Zscheischler, J.  
(2024). Direct and lagged climate change effects intensified the 2022 European drought. *Nature Geoscience*,  
17(11), 1100–1107. <https://doi.org/10.1038/s41561-024-01559-2>
- Bigler, C., & Vitasse, Y. (2021). Premature leaf discoloration of European deciduous trees is caused by drought and heat in  
515 late spring and cold spells in early fall. *Agricultural and Forest Meteorology*, 307, 108492.  
<https://doi.org/10.1016/j.agrformet.2021.108492>
- Blickensdörfer, L., Oehmichen, K., Pflugmacher, D., Kleinschmit, B., & Hostert, P. (2024). National tree species mapping  
using Sentinel-1/2 time series and German National Forest Inventory data. *Remote Sensing of Environment*, 304,  
114069. <https://doi.org/10.1016/j.rse.2024.114069>



- 520 Bose, A. K., Scherrer, D., Camarero, J. J., Ziche, D., Babst, F., Bigler, C., Bolte, A., Dorado-Liñán, I., Etzold, S., Fonti, P.,  
Forrester, D. I., Gavinet, J., Gazol, A., de Andrés, E. G., Karger, D. N., Lebourgeois, F., Lévesque, M., Martínez-  
Sancho, E., Menzel, A., ... Rigling, A. (2021). Climate sensitivity and drought seasonality determine post-drought  
growth recovery of *Quercus petraea* and *Quercus robur* in Europe. *Science of The Total Environment*, 784, 147222.  
<https://doi.org/10.1016/j.scitotenv.2021.147222>
- 525 Braun, S., Hopf, S.-E., Tresch, S., Remund, J., & Schindler, C. (2021). 37 Years of Forest Monitoring in Switzerland:  
Drought Effects on *Fagus sylvatica*. *Frontiers in Forests and Global Change*, 4.  
<https://doi.org/10.3389/ffgc.2021.765782>
- Bréda, N., Huc, R., Granier, A., & Dreyer, E. (2006). Temperate forest trees and stands under severe drought: A review of  
ecophysiological responses, adaptation processes and long-term consequences. *Annals of Forest Science*, 63(6),  
530 625–644. <https://doi.org/10.1051/forest:2006042>
- Brun, P., Psomas, A., Ginzler, C., Thuiller, W., Zappa, M., & Zimmermann, N. E. (2020). Large-scale early-wilting response  
of Central European forests to the 2018 extreme drought. *Global Change Biology*, 26(12), 7021–7035.  
<https://doi.org/10.1111/gcb.15360>
- Buras, A., Rammig, A., & Zang, C. S. (2020). Quantifying impacts of the 2018 drought on European ecosystems in  
535 comparison to 2003. *Biogeosciences*, 17(6), 1655–1672. <https://doi.org/10.5194/bg-17-1655-2020>
- Cochard, H., Bréda, N., Granier, A., & Aussenac, G. (1992). Vulnerability to air embolism of three European oak species  
(*Quercus petraea* (Matt) Liebl, *Q pubescens* Willd, *Q robur* L). *Annales Des Sciences Forestières*, 49(3), 225–233.  
<https://doi.org/10.1051/forest:19920302>
- Copernicus. (2024). *Tree Cover Density 2018—Present (raster 10m), Europe, yearly, Nov. 2024*. Copernicus Land  
540 Monitoring Service. <https://doi.org/10.2909/e677441e-fb94-431c-b4f9-304f10e4dfd8>
- De Frenne, P., Lenoir, J., Luoto, M., Scheffers, B. R., Zellweger, F., Aalto, J., Ashcroft, M. B., Christiansen, D. M., Decocq,  
G., De Pauw, K., Govaert, S., Greiser, C., Gril, E., Hampe, A., Jucker, T., Klinges, D. H., Koelemeijer, I. A.,  
Lembrechts, J. J., Marrec, R., ... Hylander, K. (2021). Forest microclimates and climate change: Importance,  
drivers and future research agenda. *Global Change Biology*, 27(11), 2279–2297. <https://doi.org/10.1111/gcb.15569>



- 545 Descals, A., Verger, A., Yin, G., Filella, I., & Peñuelas, J. (2023). Widespread drought-induced leaf shedding and legacy effects on productivity in European deciduous forests. *Remote Sensing in Ecology and Conservation*, 9(1), 76–89. <https://doi.org/10.1002/rse2.296>
- DWD. (2024). *HOSTRADA - High-resolution grids of hourly variables for Germany, Version 1.0* [Dataset]. [https://opendata.dwd.de/climate\\_environment/CDC/grids\\_germany/hourly/hostrada/](https://opendata.dwd.de/climate_environment/CDC/grids_germany/hourly/hostrada/)
- 550 Etzold, S., Sterck, F., Bose, A. K., Braun, S., Buchmann, N., Eugster, W., Gessler, A., Kahmen, A., Peters, R. L., Vitasse, Y., Walthert, L., Ziemińska, K., & Zweifel, R. (2022). Number of growth days and not length of the growth period determines radial stem growth of temperate trees. *Ecology Letters*, 25(2), 427–439. <https://doi.org/10.1111/ele.13933>
- FAWF. (2022). *Waldzustandsbericht 2022*. Forschungsanstalt für Waldökologie und Forstwirtschaft Rheinland-Pfalz, 555 Ministerium für Klimaschutz, Umwelt, Energie und Mobilität. <https://mkuem.rlp.de/service/publikationen/details/publikation/waldzustandsbericht-2022>
- Fleck, S., Cools, N., De Vos, B., Meesenburg, H., & Fischer, R. (2016). The Level II aggregated forest soil condition database links soil physicochemical and hydraulic properties with long-term observations of forest condition in Europe. *Annals of Forest Science*, 73(4), 945–957. <https://doi.org/10.1007/s13595-016-0571-4>
- 560 Frantz, D. (2019). FORCE—Landsat + Sentinel-2 Analysis Ready Data and Beyond. *Remote Sensing*, 11(9), Article 9. <https://doi.org/10.3390/rs11091124>
- Frantz, D. (2020a). *Parameterization—FORCE 3.0 documentation*. <https://force-eo.readthedocs.io/en/latest/components/higher-level/tsa/param.html>
- Frantz, D. (2020b). *Time Series Analysis—FORCE 3.0 documentation*. <https://force-eo.readthedocs.io/en/latest/components/higher-level/tsa/>
- 565 Frei, E. R., Gossner, M. M., Vitasse, Y., Queloz, V., Dubach, V., Gessler, A., Ginzler, C., Hagedorn, F., Meusburger, K., Moor, M., Samblás Vives, E., Rigling, A., Uitentuis, I., von Arx, G., & Wohlgemuth, T. (2022). European beech dieback after premature leaf senescence during the 2018 drought in northern Switzerland. *Plant Biology*, 24(7), 1132–1145. <https://doi.org/10.1111/plb.13467>



- 570 Fu, Y. S. H., Campioli, M., Vitasse, Y., De Boeck, H. J., Van den Berge, J., AbdElgawad, H., Asard, H., Piao, S., Deckmyn, G., & Janssens, I. A. (2014). Variation in leaf flushing date influences autumnal senescence and next year's flushing date in two temperate tree species. *Proceedings of the National Academy of Sciences*, *111*(20), 7355–7360. <https://doi.org/10.1073/pnas.1321727111>
- FVA-BW. (2018). *Waldzustandsbericht 2018*. Forstliche Versuchs- und Forschungsanstalt Baden-Württemberg. <https://mlr.baden-wuerttemberg.de/fileadmin/redaktion/mlr/intern/dateien/publikationen/Wald/Waldzustandsbericht2018.pdf>
- 575 FVA-BW. (2022). *Waldzustandsbericht 2022*. Forstliche Versuchs- und Forschungsanstalt Baden-Württemberg. <https://www.fva-bw.de/fileadmin/publikationen/wzb/wzb2022.pdf>
- FVA-BW. (2023). *Waldzustandsbericht 2023*. Forstliche Versuchs- und Forschungsanstalt Baden-Württemberg. [https://www.fva-bw.de/fileadmin/publikationen/wzb/wzb2023\\_Internet.pdf](https://www.fva-bw.de/fileadmin/publikationen/wzb/wzb2023_Internet.pdf)
- 580 George, J.-P., Bürkner, P.-C., Sanders, T. G. M., Neumann, M., Cammalleri, C., Vogt, J. V., & Lang, M. (2022). Long-term forest monitoring reveals constant mortality rise in European forests. *Plant Biology*, *24*(7), 1108–1119. <https://doi.org/10.1111/plb.13469>
- Gessler, A., Bächli, L., Rouholahnejad Freund, E., Treydte, K., Schaub, M., Haeni, M., Weiler, M., Seeger, S., Marshall, J., Hug, C., Zweifel, R., Hagedorn, F., Rigling, A., Saurer, M., & Meusburger, K. (2022). Drought reduces water uptake in beech from the drying topsoil, but no compensatory uptake occurs from deeper soil layers. *The New Phytologist*, *233*(1), 194–206. <https://doi.org/10.1111/nph.17767>
- 585 Gosling, R. H., Jackson, R. W., Elliot, M., & Nichols, C. P. (2024). Oak declines: Reviewing the evidence for causes, management implications and research gaps. *Ecological Solutions and Evidence*, *5*(4), e12395. <https://doi.org/10.1002/2688-8319.12395>
- 590 Grossiord, C., Buckley, T. N., Cernusak, L. A., Novick, K. A., Poulter, B., Siegwolf, R. T. W., Sperry, J. S., & McDowell, N. G. (2020). Plant responses to rising vapor pressure deficit. *New Phytologist*, *226*(6), 1550–1566. <https://doi.org/10.1111/nph.16485>



- Günthardt-Goerg, M. S., Kuster, T. M., Arend, M., & Vollenweider, P. (2013). Foliage response of young central European oaks to air warming, drought and soil type. *Plant Biology*, *15*(s1), 185–197. <https://doi.org/10.1111/j.1438-8677.2012.00665.x>
- Hájíčková, M., Plichta, R., Volařík, D., Urban, J., Matoušková, M., & Gebauer, R. (2024). Xylem function and leaf physiology in European beech saplings during and after moderate and severe drought stress. *Forestry: An International Journal of Forest Research*, *97*(2), 213–222. <https://doi.org/10.1093/forestry/cpad032>
- 600 Hammel, K., & Kennel, M. (2001). *Charakterisierung und Analyse der Wasserverfügbarkeit und des Wasserhaushalts von Waldstandorten in Bayern mit dem Simulationsmodell BROOK90* (Bd. 185). <https://library.wur.nl/WebQuery/titel/1644175>
- Haynes, K. J., Liebhold, A. M., Lefcheck, J. S., Morin, R. S., & Wang, G. (2022). Climate affects the outbreaks of a forest defoliator indirectly through its tree hosts. *Oecologia*, *198*(2), 407–418. <https://doi.org/10.1007/s00442-022-05123-w>
- 605 Jonard, F., André, F., Ponette, Q., Vincke, C., & Jonard, M. (2011). Sap flux density and stomatal conductance of European beech and common oak trees in pure and mixed stands during the summer drought of 2003. *Journal of Hydrology*, *409*(1), 371–381. <https://doi.org/10.1016/j.jhydrol.2011.08.032>
- Karolewski, P., Grzebyta, J., Oleksyn, J., & Giertych, M. J. (2007). Effects of temperature on larval survival rate and duration of development in *Lymantria monacha* (L.) on needles of *Pinus sylvestris* (L.) and in *L. dispar* (L.) on leaves of *Quercus robur* (L.). *Polish Journal of Ecology*, *55*(3), 595–600.
- Klein, T. (2014). The variability of stomatal sensitivity to leaf water potential across tree species indicates a continuum between isohydric and anisohydric behaviours. *Functional Ecology*, *28*(6), 1313–1320. <https://doi.org/10.1111/1365-2435.12289>
- 615 Klesse, S., Wohlgemuth, T., Meusburger, K., Vitasse, Y., von Arx, G., Levesque, M., Neycken, A., Braun, S., Dubach, V., Gessler, A., Ginzler, C., Gossner, M. M., Hagedorn, F., Queloz, V., Samblas Vives, E., Rigling, A., & Frei, E. R. (2022). Long-term soil water limitation and previous tree vigor drive local variability of drought-induced crown



- dieback in *Fagus sylvatica*. *SCIENCE OF THE TOTAL ENVIRONMENT*, 851, 157926.  
<https://doi.org/10.1016/j.scitotenv.2022.157926>
- 620 Knutzen, F., Averbeck, P., Barrasso, C., Bouwer, L. M., Gardiner, B., Grünzweig, J. M., Hänel, S., Haustein, K., Johannessen, M. R., Kollet, S., Müller, M. M., Pietikäinen, J.-P., Pietras-Couffignal, K., Pinto, J. G., Rechid, D., Rousi, E., Russo, A., Suarez-Gutierrez, L., Veit, S., ... Gliksmann, D. (2025). Impacts on and damage to European forests from the 2018–2022 heat and drought events. *Natural Hazards and Earth System Sciences*, 25(1), 77–117.  
<https://doi.org/10.5194/nhess-25-77-2025>
- 625 Leonova, A., Heger, A., Vázquez Navas, L. K., Jensen, K., & Reisdorff, C. (2022). Fine root mortality under severe drought reflects different root distribution of *Quercus robur* and *Ulmus laevis* trees in hardwood floodplain forests. *Trees*, 36(3), 1105–1115. <https://doi.org/10.1007/s00468-022-02275-3>
- Leuschner, C. (2020). Drought response of European beech (*Fagus sylvatica* L.)—A review. *Perspectives in Plant Ecology, Evolution and Systematics*, 47, 125576. <https://doi.org/10.1016/j.ppees.2020.125576>
- 630 Leuschner, C., Backes, K., Hertel, D., Schipka, F., Schmitt, U., Terborg, O., & Runge, M. (2001). Drought responses at leaf, stem and fine root levels of competitive *Fagus sylvatica* L. and *Quercus petraea* (Matt.) Liebl. Trees in dry and wet years. *Forest Ecology and Management*, 149(1), 33–46. [https://doi.org/10.1016/S0378-1127\(00\)00543-0](https://doi.org/10.1016/S0378-1127(00)00543-0)
- Leuschner, C., & Meier, I. C. (2018). The ecology of Central European tree species: Trait spectra, functional trade-offs, and ecological classification of adult trees. *Perspectives in Plant Ecology, Evolution and Systematics*, 33, 89–103.  
635 <https://doi.org/10.1016/j.ppees.2018.05.003>
- Leuzinger, S., Zotz, G., Asshoff, R., & Körner, C. (2005). Responses of deciduous forest trees to severe drought in Central Europe. *Tree Physiology*, 25(6), 641–650. <https://doi.org/10.1093/treephys/25.6.641>
- LFE. (2019). *Waldzustandsbericht 2019*. Landesbetrieb Forst Brandenburg, Landeskompetenzzentrum Forst Eberswalde.  
[http://www.forstliche-umweltkontrolle-bb.de/info/wze2019\\_bb.pdf](http://www.forstliche-umweltkontrolle-bb.de/info/wze2019_bb.pdf)
- 640 LFE. (2022). *Waldzustandsbericht 2022*. Landesbetrieb Forst Brandenburg, Landeskompetenzzentrum Forst Eberswalde.  
<https://mleuv.brandenburg.de/sixcms/media.php/9/Waldzustandsbericht-2022.pdf>



- Li, P., Sun, M., Xiao, J., Luo, Y., Zhang, Y., Li, X., Zhou, X., & Peng, C. (2025). Rising Atmospheric CO<sub>2</sub> Alleviates Drought Impact on Autumn Leaf Senescence Over Northern Mid-High Latitudes. *Global Ecology and Biogeography*, 34(1), e13954. <https://doi.org/10.1111/geb.13954>
- 645 LM. (2019). *Waldzustandsbericht 2019*. Landesforst Mecklenburg-Vorpommern, Ministerium für Landwirtschaft und Umwelt Mecklenburg-Vorpommern. <https://www.wald-mv.de/serviceassistent/download?id=1622367>
- LM. (2022). *Waldzustandsbericht 2022*. Landesforst Mecklenburg-Vorpommern, Ministerium für Landwirtschaft und Umwelt Mecklenburg-Vorpommern. <https://www.wald-mv.de/serviceassistent/download?id=1655727>
- LM. (2023). *Waldzustandsbericht 2023*. Landesforst Mecklenburg-Vorpommern, Ministerium für Landwirtschaft und Umwelt Mecklenburg-Vorpommern. <https://www.wald-mv.de/serviceassistent/download?id=1666165>
- 650
- Lukasová, V., Vido, J., Škvareninová, J., Bičárová, S., Hlavatá, H., Borsányi, P., & Škvarenina, J. (2020). Autumn Phenological Response of European Beech to Summer Drought and Heat. *Water*, 12(9), 2610. <https://doi.org/10.3390/w12092610>
- Ma, C., Wang, X., & Wu, C. (2024). Early leaf senescence under drought conditions in the Northern hemisphere. *Agricultural and Forest Meteorology*, 358, 110231. <https://doi.org/10.1016/j.agrformet.2024.110231>
- 655
- Manzoni, S., Vico, G., Katul, G., Palmroth, S., Jackson, R. B., & Porporato, A. (2013). Hydraulic limits on maximum plant transpiration and the emergence of the safety–efficiency trade-off. *New Phytologist*, 198(1), 169–178. <https://doi.org/10.1111/nph.12126>
- Mariën, B., Dox, I., De Boeck, H. J., Willems, P., Leys, S., Papadimitriou, D., & Campioli, M. (2021). Does drought advance the onset of autumn leaf senescence in temperate deciduous forest trees? *Biogeosciences*, 18(11), 3309–3330. <https://doi.org/10.5194/bg-18-3309-2021>
- 660
- Meier, M., Vitasse, Y., Bugmann, H., & Bigler, C. (2021). Phenological shifts induced by climate change amplify drought for broad-leaved trees at low elevations in Switzerland. *Agricultural and Forest Meteorology*, 307, 108485. <https://doi.org/10.1016/j.agrformet.2021.108485>



- 665 Misra, G., Buras, A., & Menzel, A. (2016). Effects of Different Methods on the Comparison between Land Surface and  
Ground Phenology—A Methodological Case Study from South-Western Germany. *Remote Sensing*, 8(9), Article 9.  
<https://doi.org/10.3390/rs8090753>
- Nadal-Sala, D., Grote, R., Birami, B., Knüver, T., Rehschuh, R., Schwarz, S., & Ruehr, N. K. (2021). Leaf Shedding and  
Non-Stomatal Limitations of Photosynthesis Mitigate Hydraulic Conductance Losses in Scots Pine Saplings During  
670 Severe Drought Stress. *Frontiers in Plant Science*, 12. <https://doi.org/10.3389/fpls.2021.715127>
- Neycken, A., Wohlgemuth, T., Frei, E. R., Klesse, S., Baltensweiler, A., & Lévesque, M. (2024). Slower growth prior to the  
2018 drought and a high growth sensitivity to previous year summer conditions predisposed European beech to  
crown dieback. *Science of The Total Environment*, 912, 169068. <https://doi.org/10.1016/j.scitotenv.2023.169068>
- Niemczyk, M., Wrzeński, P., Szym-Borowska, I., Krajewski, S., Żytkowiak, R., & Jagodziński, A. M. (2024). Coping with  
675 extremes: Responses of *Quercus robur* L. and *Fagus sylvatica* L. to soil drought and elevated vapour pressure  
deficit. *Science of The Total Environment*, 948, 174912. <https://doi.org/10.1016/j.scitotenv.2024.174912>
- NW-FVA. (2018). *Waldzustandsbericht 2018*. Nordwestdeutsche Forstliche Versuchsanstalt. [https://www.nw-fva.de/fileadmin/nwfva/publikationen/pdf/paar\\_2018\\_waldzustandsbericht\\_2018.pdf](https://www.nw-fva.de/fileadmin/nwfva/publikationen/pdf/paar_2018_waldzustandsbericht_2018.pdf)
- NW-FVA. (2019). *Waldzustandsbericht 2019*. Nordwestdeutsche Forstliche Versuchsanstalt. [https://www.nw-fva.de/fileadmin/nwfva/publikationen/pdf/paar\\_2019\\_waldzustandsbericht\\_2019.pdf](https://www.nw-fva.de/fileadmin/nwfva/publikationen/pdf/paar_2019_waldzustandsbericht_2019.pdf)
- 680 NW-FVA. (2021). *Waldzustandsbericht 2021*. [https://www.nw-fva.de/fileadmin/nwfva/publikationen/pdf/nordwestdeutsche\\_forstliche\\_versuchsanstalt\\_2021\\_waldzustandsbericht\\_2021\\_fur\\_hessen.pdf](https://www.nw-fva.de/fileadmin/nwfva/publikationen/pdf/nordwestdeutsche_forstliche_versuchsanstalt_2021_waldzustandsbericht_2021_fur_hessen.pdf)
- Obladen, N., Dechering, P., Skiadareisis, G., Tegel, W., Keßler, J., Höllerl, S., Kaps, S., Hertel, M., Dulamsuren, C., Seifert,  
685 T., Hirsch, M., & Seim, A. (2021). Tree mortality of European beech and Norway spruce induced by 2018-2019 hot  
droughts in central Germany. *Agricultural and Forest Meteorology*, 307, 108482.  
<https://doi.org/10.1016/j.agrformet.2021.108482>



- Piao, S., Liu, Q., Chen, A., Janssens, I. A., Fu, Y., Dai, J., Liu, L., Lian, X., Shen, M., & Zhu, X. (2019). Plant phenology and global climate change: Current progresses and challenges. *Global Change Biology*, 25(6), 1922–1940.  
690 <https://doi.org/10.1111/gcb.14619>
- Pietig, K., Kotowska, M., Coners, H., Mundry, R., & Leuschner, C. (2026). Deep rooting revisited: Comparing the rooting patterns of European beech, Sessile oak, Scots pine, and Douglas fir in sandy soil to 3.8 m depth. *Forest Ecology and Management*, 600(123288), 1–14. <https://doi.org/10.1016/j.foreco.2025.123288>
- Plotkin, A. B., Blumstein, M., Laflower, D., Pasquarella, V. J., Chandler, J. L., Elkinton, J. S., & Thompson, J. R. (2021). Defoliated trees die below a critical threshold of stored carbon. *Functional Ecology*, 35(10), 2156–2167.  
695 <https://doi.org/10.1111/1365-2435.13891>
- Quetin, G. R., Anderegg, L. D. L., & Trugman, A. T. (2026). Leaf Shedding During Drought Reduces Hydraulic Stress in Trees. *AGU Advances*, 7(2), e2025AV001907. <https://doi.org/10.1029/2025AV001907>
- Rakovec, O., Samaniego, L., Hari, V., Markonis, Y., Moravec, V., Thober, S., Hanel, M., & Kumar, R. (2022). The 2018–  
700 2020 Multi-Year Drought Sets a New Benchmark in Europe. *Earth's Future*, 10(3), e2021EF002394.  
<https://doi.org/10.1029/2021EF002394>
- Raspe, S., Fleck, S., Beuker, E., Bastrup-Birk, A., & Preuhsler, T. (2020). Part VI: Phenological Observations. Version 2020-3. In UNECE ICP Forests Programme Co-ordinating Centre (Hrsg.), *Manual on methods and criteria for harmonized sampling, assessment, monitoring and analysis of the effects of air pollution on forests*. Thünen  
705 Institute of Forest Ecosystems. [https://www.icp-forests.net/fileadmin/icp\\_forests/Dateien/Manual\\_Versions/2020-22/ICP\\_Manual\\_part06\\_2020\\_Phenology\\_version\\_2020-4.pdf](https://www.icp-forests.net/fileadmin/icp_forests/Dateien/Manual_Versions/2020-22/ICP_Manual_part06_2020_Phenology_version_2020-4.pdf)
- Richardson, A. D., Keenan, T. F., Migliavacca, M., Ryu, Y., Sonnentag, O., & Toomey, M. (2013). Climate change, phenology, and phenological control of vegetation feedbacks to the climate system. *Agricultural and Forest Meteorology*, 169, 156–173. <https://doi.org/10.1016/j.agrformet.2012.09.012>
- 710 Rodríguez-Calcerrada, J., Sancho-Knapik, D., Martin-StPaul, N. K., Limousin, J.-M., McDowell, N. G., & Gil-Pelegrín, E. (2017). Drought-Induced Oak Decline—Factors Involved, Physiological Dysfunctions, and Potential Attenuation by Forestry Practices. In E. Gil-Pelegrín, J. J. Peguero-Pina, & D. Sancho-Knapik (Hrsg.), *Oaks Physiological*



*Ecology. Exploring the Functional Diversity of Genus Quercus L.* (S. 419–451). Springer International Publishing.

[https://doi.org/10.1007/978-3-319-69099-5\\_13](https://doi.org/10.1007/978-3-319-69099-5_13)

715 Salmon, Y., Torres-Ruiz, J. M., Poyatos, R., Martinez-Vilalta, J., Meir, P., Cochard, H., & Mencuccini, M. (2015). Balancing the risks of hydraulic failure and carbon starvation: A twig scale analysis in declining Scots pine. *Plant, Cell & Environment*, 38(12), 2575–2588. <https://doi.org/10.1111/pce.12572>

SBS. (2018). *Waldzustandsbericht 2018*. Staatsbetrieb Sachsenforst, Sächsisches Staatsministerium für Umwelt und Landwirtschaft. <https://publikationen.sachsen.de/bdb/artikel/32379>

720 Scafaro, A. P., Fan, Y., Posch, B. C., Garcia, A., Coast, O., & Atkin, O. K. (2021). Responses of leaf respiration to heatwaves. *Plant, Cell & Environment*, 44(7), 2090–2101. <https://doi.org/10.1111/pce.14018>

Scharnweber, T., Manthey, M., & Wilmking, M. (2013). Differential radial growth patterns between beech (*Fagus sylvatica* L.) and oak (*Quercus robur* L.) on periodically waterlogged soils. *Tree Physiology*, 33(4), 425–437. <https://doi.org/10.1093/treephys/tpt020>

725 Schiefer, F., Schmidlein, S., Hartmann, H., Schnabel, F., & Kattenborn, T. (2025). Large-scale remote sensing reveals that tree mortality in Germany appears to be greater than previously expected. *Forestry: An International Journal of Forest Research*, 98(4), 535–549. <https://doi.org/10.1093/forestry/cpae062>

Schmidt-Walter, P., Ahrends, B., Mette, T., Puhlmann, H., & Meesenburg, H. (2019). NFIWADS: The water budget, soil moisture, and drought stress indicator database for the German National Forest Inventory (NFI). *Annals of Forest Science*, 76(2), Article 2. <https://doi.org/10.1007/s13595-019-0822-2>

730 Schmidt-Walter, P., Trotsiuk, V., Meusburger, K., Zacios, M., & Meesenburg, H. (2020). Advancing simulations of water fluxes, soil moisture and drought stress by using the LWF-Brook90 hydrological model in R. *Agricultural and Forest Meteorology*, 291, 108023. <https://doi.org/10.1016/j.agrformet.2020.108023>

Schuldt, B., Buras, A., Arend, M., Vitasse, Y., Beierkuhnlein, C., Damm, A., Gharun, M., Grams, T. E. E., Hauck, M.,  
735 Hajek, P., Hartmann, H., Hiltbrunner, E., Hoch, G., Holloway-Phillips, M., Körner, C., Larysch, E., Lübke, T.,  
Nelson, D. B., Rammig, A., ... Kahmen, A. (2020). A first assessment of the impact of the extreme 2018 summer



- drought on Central European forests. *Basic and Applied Ecology*, 45, 86–103.  
<https://doi.org/10.1016/j.baae.2020.04.003>
- 740 Schwieder, M., Leitão, P. J., da Cunha Bustamante, M. M., Ferreira, L. G., Rabe, A., & Hostert, P. (2016). Mapping  
Brazilian savanna vegetation gradients with Landsat time series. *International Journal of Applied Earth  
Observation and Geoinformation*, 52, 361–370. <https://doi.org/10.1016/j.jag.2016.06.019>
- Spieß, N., Oufir, M., Matušíková, I., Stierschneider, M., Kopecky, D., Homolka, A., Burg, K., Fluch, S., Hausman, J.-F., &  
Wilhelm, E. (2012). Ecophysiological and transcriptomic responses of oak (*Quercus robur*) to long-term drought  
exposure and rewatering. *Environmental and Experimental Botany*, 77, 117–126.  
745 <https://doi.org/10.1016/j.envexpbot.2011.11.010>
- Spinoni, J., Vogt, J. V., Naumann, G., Barbosa, P., & Dosio, A. (2018). Will drought events become more frequent and  
severe in Europe? *International Journal of Climatology*, 38(4), 1718–1736. <https://doi.org/10.1002/joc.5291>
- Tanzer, D. N., Bagchi, R., Plotkin, A. B., Mickley, J., Rivers, K. J., Sagarin, M., & Fahey, R. T. (2025). Defoliation  
frequency outweighs timing as a driver of tree mortality related to drought-defoliation interaction. *Forest Ecology  
and Management*, 592, 122859. <https://doi.org/10.1016/j.foreco.2025.122859>
- 750 TMIL. (2018). *Waldzustandsbericht 2018*. Thüringer Ministerium für Infrastruktur und Landwirtschaft. [https://digitales-  
infrastruktur.thueringen.de/fileadmin/Forst\\_und\\_Jagd\\_Fischerei/Forstwirtschaft/2018\\_Waldzustandsbericht\\_web.pdf](https://digitales-<br/>infrastruktur.thueringen.de/fileadmin/Forst_und_Jagd_Fischerei/Forstwirtschaft/2018_Waldzustandsbericht_web.pdf)  
f
- TMIL. (2020). *Waldzustandsbericht 2019*. Thüringer Ministerium für Infrastruktur und Landwirtschaft.  
755 [https://umwelt.thueringen.de/fileadmin/Forst\\_und\\_Jagd\\_Fischerei/Forstwirtschaft/2019\\_Waldzustandsbericht.pdf](https://umwelt.thueringen.de/fileadmin/Forst_und_Jagd_Fischerei/Forstwirtschaft/2019_Waldzustandsbericht.pdf)
- Vander Mijnsbrugge, K., Turcsán, A., Maes, J., Duchêne, N., Meeus, S., Steppe, K., & Steenackers, M. (2016). Repeated  
Summer Drought and Re-watering during the First Growing Year of Oak (*Quercus petraea*) Delay Autumn  
Senescence and Bud Burst in the Following Spring. *Frontiers in Plant Science*, 7, 419.  
<https://doi.org/10.3389/fpls.2016.00419>
- 760 Vanhellemont, M., Sousa-Silva, R., Maes, S. L., Van den Bulcke, J., Hertzog, L., De Groote, S. R. E., Van Acker, J., Bonte,  
D., Martel, A., Lens, L., & Verheyen, K. (2019). Distinct growth responses to drought for oak and beech in



temperate mixed forests. *Science of The Total Environment*, 650, 3017–3026.

<https://doi.org/10.1016/j.scitotenv.2018.10.054>

765 Wald und Holz NRW. (2021). *Waldzustandsbericht 2021*. Landesbetrieb Wald und Holz Nordrhein-Westfalen, Ministerium für Umwelt, Landwirtschaft, Natur- und Verbraucherschutz des Landes Nordrhein-Westfalen. [https://www.wald-und-holz.nrw.de/fileadmin/Wald\\_in\\_NRW/Waldzustandsbericht\\_NRW\\_2021\\_Langfassung.pdf](https://www.wald-und-holz.nrw.de/fileadmin/Wald_in_NRW/Waldzustandsbericht_NRW_2021_Langfassung.pdf)

770 Walthert, L., Ganthaler, A., Mayr, S., Saurer, M., Waldner, P., Walser, M., Zweifel, R., & von Arx, G. (2021). From the comfort zone to crown dieback: Sequence of physiological stress thresholds in mature European beech trees across progressive drought. *Science of The Total Environment*, 753, 141792. <https://doi.org/10.1016/j.scitotenv.2020.141792>

775 Weis, W., Ahrends, B., Böhner, J., Falk, W., Fleck, S., Habel, R., Klemmt, H.-J., Meesenburg, H., Müller, A.-C., Puhlmann, H., Wehberg, J.-A., Wellpott, A., & Wolf, T. (with Bayerische Landesanstalt für Wald und Forstwirtschaft, Nordwestdeutsche Forstliche Versuchsanstalt, Forstliche Versuchs- und Forschungsanstalt Baden-Württemberg, Universität Hamburg, Scilands GmbH, & Zentrum Wald - Forst - Holz Weihenstephan). (2023). *Standortsfaktor Wasserhaushalt im Klimawandel (WHH-KW): Abschlussveröffentlichung zum Forschungsprojekt, Teilprojekte 01, 02, 03, 04*. Zentrum Wald Forst Holz Weihenstephan.

780 Wohlgemuth, T., Kistler, M., Aymon, C., Hagedorn, F., Gessler, A., Gossner, M. M., Queloz, V., Vögli, I., Wasem, U., Vitasse, Y., & Rigling, A. (2020). Früher Laubfall der Buche während der Sommertrockenheit 2018: Resistenz oder Schwächesymptom? *Schweizerische Zeitschrift für Forstwesen*, 171(5), 257–269. <https://doi.org/10.3188/szf.2020.0257>

Wolfe, B. T., Sperry, J. S., & Kursar, T. A. (2016). Does leaf shedding protect stems from cavitation during seasonal droughts? A test of the hydraulic fuse hypothesis. *New Phytologist*, 212(4), 1007–1018. <https://doi.org/10.1111/nph.14087>

785 Yan, W., Zhou, J., Lin, H., Luo, J., Duan, X., & Wu, R. (2025). Drivers of the pre-season drought thresholds triggering earlier autumn foliar senescence in the Northern Hemisphere. *Nature Communications*, 16(1), 7568. <https://doi.org/10.1038/s41467-025-62847-y>



- Zani, D., Crowther, T. W., Mo, L., Renner, S. S., & Zohner, C. M. (2020). Increased growing-season productivity drives earlier autumn leaf senescence in temperate trees. *Science*, 370(6520), 1066–1071. <https://doi.org/10.1126/science.abd8911>
- 790 Zhang, X., Wang, X., Zohner, C. M., Peñuelas, J., Li, Y., Wu, X., Zhang, Y., Liu, H., Shen, P., Jia, X., Liu, W., Tian, D., Pradhan, P., Fandohan, A. B., Peng, D., & Wu, C. (2025). Declining precipitation frequency may drive earlier leaf senescence by intensifying drought stress and enhancing drought acclimation. *Nature Communications*, 16(1), 910. <https://doi.org/10.1038/s41467-025-56159-4>
- Zuccarini, P., Delpierre, N., Mariën, B., Peñuelas, J., Heinecke, T., & Campioli, M. (2023). Drivers and dynamics of foliar senescence in temperate deciduous forest trees at their southern limit of distribution in Europe. *Agricultural and Forest Meteorology*, 342, 109716. <https://doi.org/10.1016/j.agrformet.2023.109716>
- 795